



Role of chlorohydrocarbon in increasing selectivity of propylene oxide over Ag–Y₂O₃–K₂O/α-Al₂O₃ catalyst for epoxidation of propylene by molecular oxygen

Wei Yao^{a,b}, Xiang Zheng^a, Yanglong Guo^{a,*}, Wangcheng Zhan^a, Yun Guo^a, Guanzhong Lu^{a,*}

^a Key Laboratory for Advanced Materials, Research Institute of Industrial Catalysis, East China University of Science and Technology, 130 Meilong Road, Shanghai 200237, PR China

^b National Engineering Research Center for Nanotechnology, Shanghai 200241, PR China

ARTICLE INFO

Article history:

Received 11 February 2011

Received in revised form 2 April 2011

Accepted 6 April 2011

Available online 13 April 2011

Keywords:

Epoxidation of propylene

Molecular oxygen

Propylene oxide

Silver-based catalyst

Chlorohydrocarbon

ABSTRACT

Effects of concentration of chlorohydrocarbon and reaction time on the catalytic performance of 20% Ag–0.1% Y₂O₃–0.1% K₂O/α-Al₂O₃ catalyst for the epoxidation of propylene by molecular oxygen were investigated, in which the role of chlorohydrocarbon in increasing selectivity of propylene oxide (PO) was characterized by XRD, SEM-EDS and XPS. With an increase in the concentration of chlorohydrocarbon in the feed gas, PO selectivity increased significantly and propylene conversion decreased remarkably and then the catalytic performance remained nearly constant when the concentration of chlorohydrocarbon was more than 125 ppm. PO selectivity increased from 46.8% to 75.6% and propylene conversion declined from 4.0% to 0.77% after 10 h induction period, and then the catalytic performance remained nearly constant for 140 h, under the reaction conditions of 245 °C, 0.1 MPa, GHSV of 2000 h⁻¹, and 125 ppm 1,1,1-trichloroethane (TCE). A small amount of TCE could effectively control the surface morphology of the catalyst and restrain the agglomeration of Ag crystallites, in which TCE was dissociated on the surface of Ag crystallites to form AgCl and the coexistence of Ag and AgCl was favorable to increase PO selectivity. The presence of Cl could withdraw electrons from nearby Ag and thus make Ag electropositive, which was beneficial to produce more active sites where electrophilic oxygen species could be absorbed to increase PO selectivity. Y₂O₃ played a role of electron-type promoter that could strongly polarize electron cloud of nearby Ag, which made the absorbed oxygen species hold proper electrophilic character and then attack C=C bond of propylene to produce PO.

© 2011 Elsevier B.V. All rights reserved.

1. Introduction

Propylene oxide (PO) is an important intermediate in the chemical industry. The major applications of PO are the manufacture of polyether polyols, propylene glycol and nonionic surfactants. Propylene oxide is generally produced by the chlorohydrin process and the Halcon process [1]. The major drawback of the chlorohydrin process is that it requires a large deal of chlorine, which is expensive, toxic and erosive. Moreover, some chlorinated by-products also result in the serious environmental problems. In the Halcon process, PO is produced together with the equimolar amount of co-product which value depends on its demand in the market. In the past few years, hydrogen peroxide to propylene oxide (HPPO) technology has been developed by BASF AG and Dow Chemical for the epoxidation of propylene, which frees PO from the creation of co-products or from heavy integration with chlor-alkali production, but the cost of hydrogen peroxide is too high for the production of bulk chemicals like PO [2,3].

Many studies have been carried out for the gas-phase epoxidation of propylene by molecular oxygen to meet the requirements of green chemistry and low cost for production of PO. PO selectivity of 65% and propylene conversion of 15% were obtained over the molten salt catalysts, however, the reaction was extremely sensitive to the reactor and operation conditions, and hence the catalytic performance was very difficult to repeat [4–7]. Nitrous oxide can produce the suitable electrophilic oxygen species to attack the C=C bond of propylene to produce PO, propanal and acetone, in which high temperature, acidic or basic conditions are in favor of isomerization of PO to propanal and acetone. Sodium promoted iron oxide/SiO₂ catalyst could catalyze the gas-phase oxidation of propylene with nitrous oxide as the oxidant, in which PO selectivity of 40–60% and propylene conversion of 6–12% were achieved [8]. CuOx/SBA-15 or Cu/SiO₂ catalyst after K modification exhibited better catalytic performance for the epoxidation of propylene by molecular oxygen [9–12].

Many epoxidation reactions over Ag-based catalysts and simulation studies on the interaction of oxygen with Ag surfaces were investigated. An excellent review about these studies was published [13]. Moreover, many researchers strived to carry out the epoxidation of propylene over Ag-based catalysts with bet-

* Corresponding authors. Tel.: +86 21 64252923; fax: +86 21 64252923.
E-mail addresses: ylguo@ecust.edu.cn (Y. Guo), gzhlu@ecust.edu.cn (G. Lu).

ter catalytic performance. Unfortunately, both PO selectivity and propylene conversion were less than 15% [14]. Previous studies indicated that lower PO selectivity was due to the more easily connecting of allylic hydrogen with the adsorbed oxygen species to form the conjugate-stabilized allyl radical or anion which was easily further oxidized to CO_2 and H_2O [15–19]. If the modified silver-based catalyst could produce the mild electrophilic oxygen species to attack the $\text{C}=\text{C}$ bond of propylene, the catalyst would be highly effective for the epoxidation reaction. Oxygen conversion of 6.8% and PO selectivity of 53.1% were attained over $\text{Ag}-\text{MoO}_3/\text{ZrO}_2$ catalyst [20,21]. Propylene conversion of 4.0% and PO selectivity of 46.8% were achieved over $\text{Ag}-\text{Y}_2\text{O}_3-\text{K}_2\text{O}/\alpha-\text{Al}_2\text{O}_3$ catalyst [22,23]. Propylene conversion of 54% and PO selectivity of 26.3% with air as the oxidant were attained over unsupported Ag catalysts promoted with NaCl or BaCl_2 [24]. Propylene conversion of 1.64% and PO selectivity of 30.6% were achieved over $\text{Ag}-\text{CuCl}$ (1/0.6) catalyst [25].

In this paper, effects of concentration of chlorohydrocarbon and reaction time on the catalytic performance of $\text{Ag}-\text{Y}_2\text{O}_3-\text{K}_2\text{O}/\alpha-\text{Al}_2\text{O}_3$ catalyst for the epoxidation of propylene by molecular oxygen were investigated, in which the role of chlorohydrocarbon in increasing PO selectivity was characterized by XRD, SEM-EDS and XPS.

2. Experimental

2.1. Preparation of catalyst

The catalyst was prepared as follows: $\alpha-\text{Al}_2\text{O}_3$ support (20–40 mesh, specific surface area of $10.3\text{ m}^2/\text{g}$) was impregnated with $\text{Y}(\text{NO}_3)_3$ and KNO_3 aqueous solution at 60°C for 1 h, dried at 120°C for 5 h, and then calcined at 550°C for 2 h. The modified $\alpha-\text{Al}_2\text{O}_3$ support was dunked into the silver–ammonium complex solution (synthesized by adding silver oxalate to ethylenediamine aqueous solution) for 0.5 h at 60°C , dried at 80°C for 2.5 h, and then calcined at 280°C for 10 min. The weight composition of catalyst was 20% $\text{Ag}-0.1\% \text{Y}_2\text{O}_3-0.1\% \text{K}_2\text{O}/\alpha-\text{Al}_2\text{O}_3$.

2.2. Epoxidation of propylene

The epoxidation of propylene was carried out in the stainless-steel fixed-bed reactor ($\phi 5 \times 360\text{ mm}$) under the reaction conditions of 245°C , 0.1 MPa and GHSV of 2000 h^{-1} . 0.5 mL $\text{Ag}-\text{Y}_2\text{O}_3-\text{K}_2\text{O}/\alpha-\text{Al}_2\text{O}_3$ catalyst was packed in the reactor and the composition of the feed gas (20% C_3H_6 , 8% O_2 , balance N_2 and 25–200 ppm chlorohydrocarbon) was controlled by three mass flow meters. The products were qualitatively identified by INFI-CON IPC400 quadrupole spectrometer. The compositions of feed gas and products were analyzed quantitatively by two on-line gas chromatographs with three packed columns (G.D.X-401, silica gel and 5A zeolite) and TCD detectors. Carbon balance was used to calculate propylene conversion and PO selectivity in the epoxidation reaction. When the fresh catalyst (a) was evaluated for 150 h without or with 125 ppm 1,1,1-trichloroethane in the feed gas, the catalyst was defined as the aged catalyst (b) or the aged catalyst (c), respectively.

2.3. Characterization of catalyst

XRD patterns were recorded on a Rigaku D/max-2550VB/PC diffractometer operated at 40 kV, 100 mA ($\text{CuK}\alpha$ radiation, $\lambda = 0.15406\text{ nm}$). The size of Ag crystallites was determined by Scherrer's equation with the full peak width at half maximum height of the diffraction peak of Ag (1 1 1). SEM-EDS were operated on a JEOL JSM-6360LV scanning electron microscope with Falcon energy dispersive spectrometer. XPS spectra were recorded

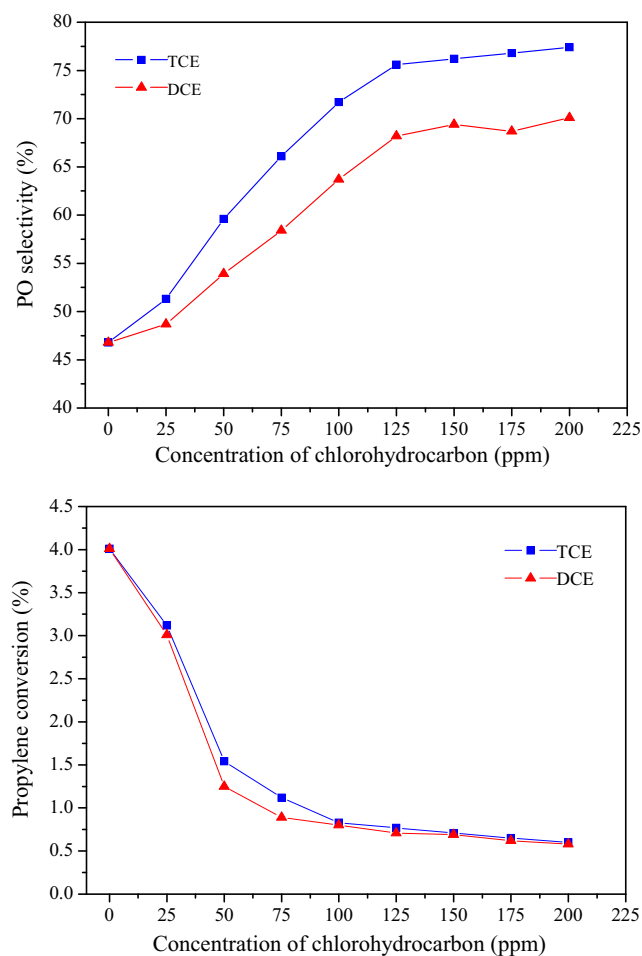


Fig. 1. Effect of concentration of chlorohydrocarbon on the catalytic performance of $\text{Ag}-\text{Y}_2\text{O}_3-\text{K}_2\text{O}/\alpha-\text{Al}_2\text{O}_3$ catalyst for the epoxidation of propylene. Reaction conditions: 0.5 mL catalyst, 245°C , 0.1 MPa, and GHSV of 2000 h^{-1} of the feed gas (20% C_3H_6 , 8% O_2 , balance N_2 and 25–200 ppm chlorohydrocarbon).

on a Thermo ESCALAB 250 spectrometer with a monochromatized $\text{AlK}\alpha$ X-ray source (1486.6 eV), and a passing energy of 20 eV. C1s (binding energy 284.6 eV) of adventitious carbon was used as the reference.

3. Results and discussion

3.1. Effect of concentration of chlorohydrocarbon

Fig. 1 shows effect of concentration of chlorohydrocarbon on the catalytic performance of $\text{Ag}-\text{Y}_2\text{O}_3-\text{K}_2\text{O}/\alpha-\text{Al}_2\text{O}_3$ catalyst for the epoxidation of propylene, in which all data were measured after 10 h induction period. As shown in Fig. 1, over $\text{Ag}-\text{Y}_2\text{O}_3-\text{K}_2\text{O}/\alpha-\text{Al}_2\text{O}_3$ catalyst, PO selectivity and propylene conversion were 46.8% and 4.0%, respectively, without chlorohydrocarbon in the feed gas. With an increase in the concentration of chlorohydrocarbon (1,1,1-trichloroethane (TCE) or 1,2-dichloroethane (DCE)) in the feed gas, PO selectivity increased significantly and propylene conversion decreased remarkably and then the catalytic performance remained nearly constant when the concentration of chlorohydrocarbon was more than 125 ppm. With an increase in the concentration of TCE up to 125 ppm, PO selectivity increased from 46.8% to 75.6%, while propylene conversion declined from 4.0% to 0.77%, which agrees well with the literature that DCE in the gas phase in ppm quantities could increase the selectivity of ethylene oxide from 48% to 75% over $\text{Ag}/\alpha-\text{Al}_2\text{O}_3$ catalyst for the epoxida-

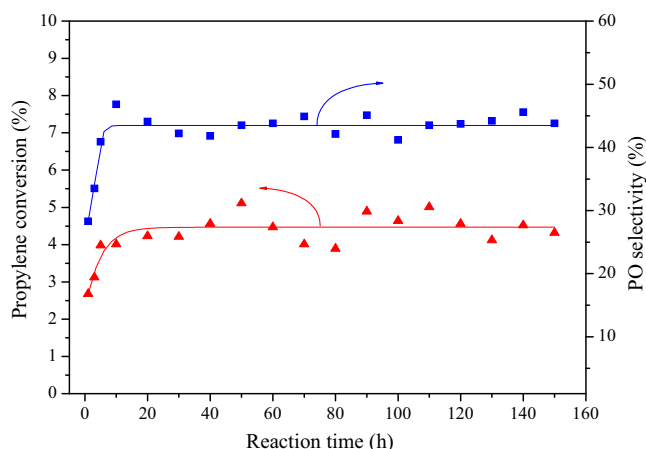


Fig. 2. Stability of Ag–Y₂O₃–K₂O/α-Al₂O₃ catalyst for the epoxidation of propylene without chlorohydrocarbon in the feed gas. Reaction conditions: 0.5 mL catalyst, 245 °C, 0.1 MPa, and GHSV of 2000 h⁻¹ of the feed gas (20% C₃H₆, 8% O₂, and balance N₂).

tion of ethylene [26]. TCE had more positive effect on PO selectivity than DCE. Due to polarization effect, C–Cl bond of TCE molecule was much easier to dissociate than that of DCE, and then Cl partially poisoned the active sites of Ag–Y₂O₃–K₂O/α-Al₂O₃ catalyst, which resulted in an increase in PO selectivity and a decrease in propylene conversion. When the concentration of chlorohydrocarbon was more than 125 ppm, Cl species adsorbed on Ag surface reached saturation and hence the catalytic performance remained nearly constant.

Fig. 2 shows stability of Ag–Y₂O₃–K₂O/α-Al₂O₃ catalyst for the epoxidation of propylene without chlorohydrocarbon in the feed gas. As shown in Fig. 2, with an increase in reaction time, PO selectivity and propylene conversion gradually increased up to 46.8% and 4.0%, respectively, after 10 h induction period, and then the catalytic performance remained nearly constant for 140 h. Fig. 3 shows stability of Ag–Y₂O₃–K₂O/α-Al₂O₃ catalyst for the epoxidation of propylene with 125 ppm TCE in the feed gas. As shown in Fig. 3, with an increase in reaction time, PO selectivity increased significantly to 75.6% and propylene conversion decreased remarkably to 0.77% after 10 h induction period, and then the catalytic performance remained nearly constant for 140 h.

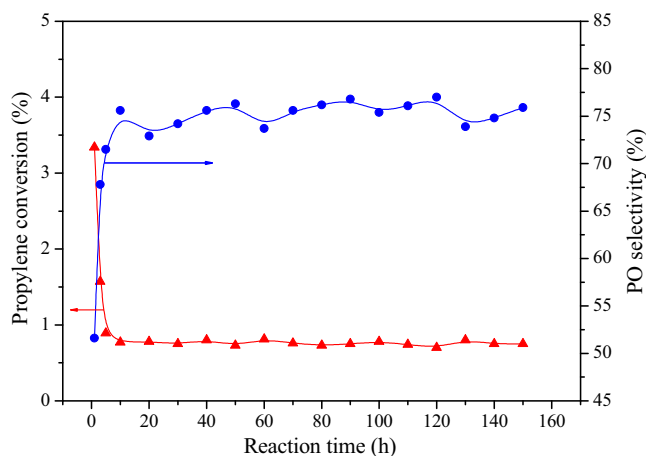


Fig. 3. Stability of Ag–Y₂O₃–K₂O/α-Al₂O₃ catalyst for the epoxidation of propylene with 125 ppm TCE in the feed gas. Reaction conditions: 0.5 mL catalyst, 245 °C, 0.1 MPa, and GHSV of 2000 h⁻¹ of the feed gas (20% C₃H₆, 8% O₂, balance N₂ and 125 ppm TCE).

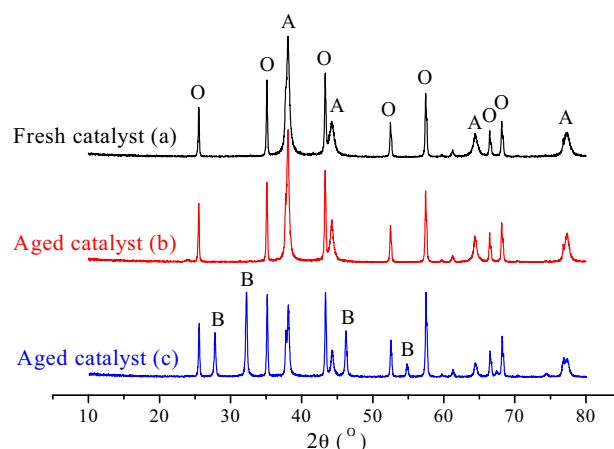


Fig. 4. XRD patterns of the fresh catalyst (a), aged catalyst (b) and aged catalyst (c) with 125 ppm TCE in the feed gas (O–α-Al₂O₃; A–Ag; B–AgCl).

3.2. Characterization of catalyst

3.2.1. XRD

Fig. 4 shows XRD patterns of the fresh catalyst (a), aged catalyst (b) and aged catalyst (c) with 125 ppm TCE in the feed gas. As shown in Fig. 4, over the fresh catalyst (a), the diffraction peaks of Y₂O₃ and K₂O could not be observed due to their low loading. The diffraction peaks of α-Al₂O₃ support located at 2θ = 25.6°, 35.2°, 43.4°, 52.6°, 57.5°, 66.5° and 68.2°. There were four diffraction peaks of Ag at 2θ = 38.1°, 44.3°, 64.4° and 77.4°, corresponding to the crystal faces of Ag (1 1 1), (2 0 0), (2 2 0) and (3 1 1), respectively. The diffraction peaks of silver oxides were not observed. When the fresh catalyst was evaluated for 150 h without 125 ppm TCE in the feed gas, over the aged catalyst (b), only the diffraction peaks of Ag and α-Al₂O₃ were observed, and the intensities of the diffraction peaks of Ag obviously increased. However, when the fresh catalyst was evaluated for 150 h with 125 ppm TCE in the feed gas, over the aged catalyst (c), the diffraction peaks of AgCl besides Ag and α-Al₂O₃ were observed, and the intensities of the diffraction peaks of Ag obviously decreased. As shown in Figs. 4 and 1, the coexistence of Ag and AgCl over Ag–Y₂O₃–K₂O/α-Al₂O₃ catalyst was favorable to increase PO selectivity. The presence of AgCl could affect the electron density of the silver atoms nearby and thus made the adsorbed oxygen species with proper electron density, which was beneficial to the epoxidation reaction [27]. The size of Ag crystallites of the fresh catalyst (a) was 15.8 nm. The size of Ag crystallites of the aged catalyst (b) increased to 17.2 nm, which was due to the sintering of Ag crystallites during the epoxidation reaction. However, the size of Ag crystallites of the aged catalyst (c) decreased to 14.7 nm, which indicated that presence of TCE could effectively promote dispersion of Ag crystallites to some extent and restrain the agglomeration of Ag crystallites.

3.2.2. SEM-EDS

In order to understand effects of chlorohydrocarbon and reaction time on the catalytic performance of Ag–Y₂O₃–K₂O/α-Al₂O₃ catalyst, their surface morphology and surface composition were determined by SEM-EDS. Fig. 5 shows SEM images of the fresh catalyst (a), aged catalyst (b) and aged catalyst (c) with 125 ppm TCE in the feed gas. As shown in Fig. 5, the surface of the fresh catalyst (a) was nonuniformly and mostly covered by small spherical Ag particles, which was attributed to the thermal decomposition of the silver–ammonium complex to form small spherical Ag particles. Over the aged catalyst (b), small spherical Ag particles became flake Ag particles, which was due to the sintering of Ag crystallites during the epoxidation reaction [28]. Over the aged catalyst (c), only a

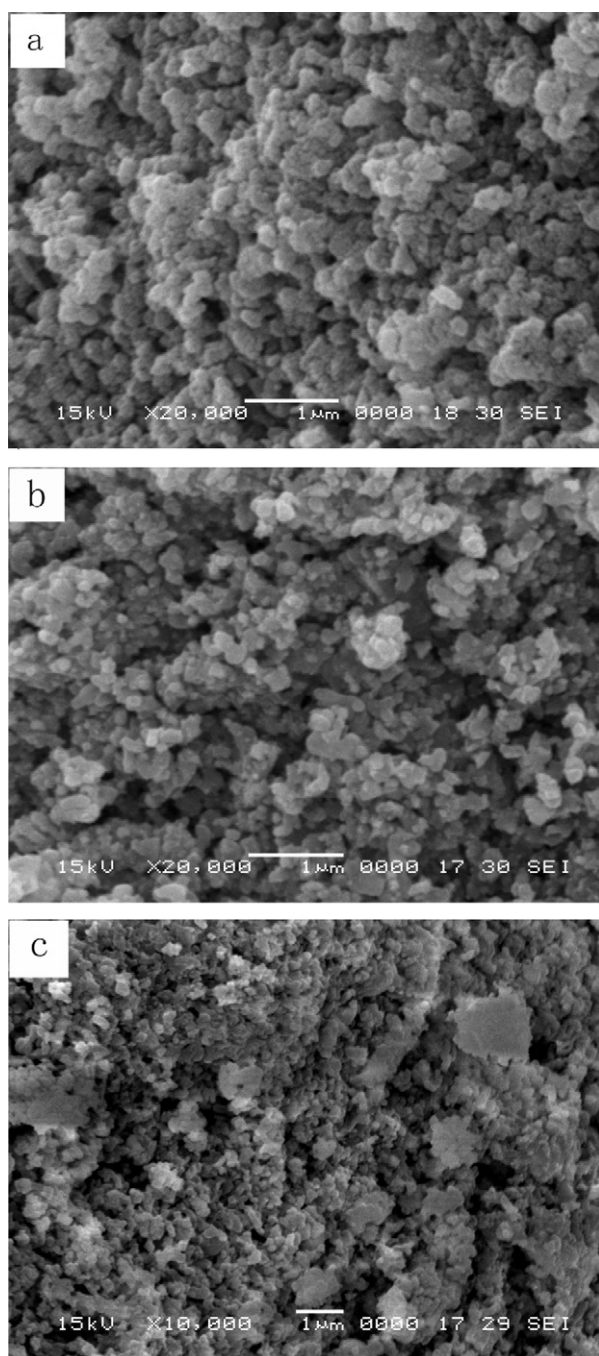


Fig. 5. SEM images of the fresh catalyst (a), aged catalyst (b) and aged catalyst (c) with 125 ppm TCE in the feed gas.

few Ag particles were sintered and the catalyst surface was mostly covered by small floccules Ag particles, which indicated that a small amount of TCE could effectively control the surface morphology of the catalyst and restrain the agglomeration of Ag crystallites.

Table 1

The surface composition (wt%) of the fresh catalyst (a), aged catalyst (b) and aged catalyst (c) with 125 ppm TCE in the feed gas determined by SEM-EDS.

Samples	Ag	Al	O	Cl
Fresh catalyst (a)	29.8	35.9	34.3	0
Aged catalyst (b)	25.1	43.1	31.8	0
Aged catalyst (c)	29.7	36.2	32.0	2.1

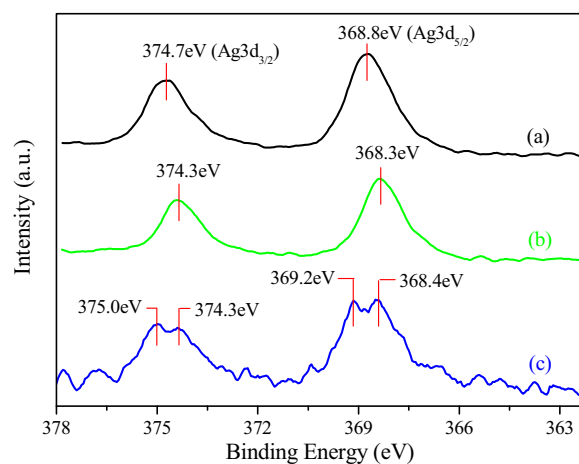


Fig. 6. Ag3d XPS spectra of the fresh catalyst (a), aged catalyst (b) and aged catalyst (c) with 125 ppm TCE in the feed gas.

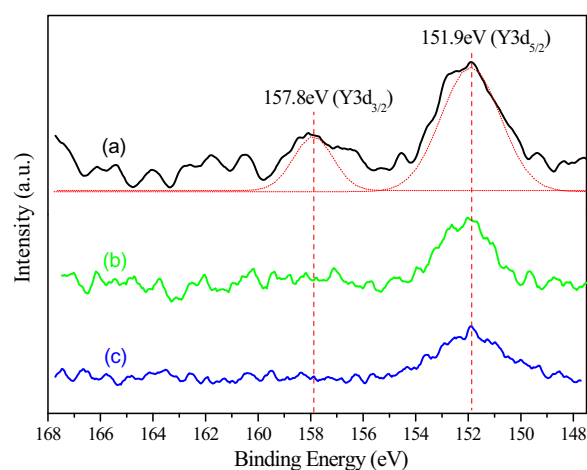


Fig. 7. Y3d XPS spectra of the fresh catalyst (a), aged catalyst (b) and aged catalyst (c) with 125 ppm TCE in the feed gas.

Table 1 shows the surface composition of the fresh catalyst (a), aged catalyst (b) and aged catalyst (c) with 125 ppm TCE in the feed gas determined by SEM-EDS. As shown in **Table 1**, Y and K were not detected due to their low loading and covering by Ag crystallites. Ag content of the aged catalyst (b) was 4.7% lower than that of the fresh catalyst (a), while its Al content was 7.2% higher than that of the fresh catalyst (a), which was attributed to the agglomeration of Ag crystallites and more exposure of α -Al₂O₃ support with an increase in reaction time. The contents of Ag and Al of the aged catalyst (c) were nearly the same as those of the fresh catalyst (a), and its Cl content was 2.1%. The presence of Cl on the surface of the aged catalyst (c) was due to dissociation of TCE in the feed gas on the surface of Ag crystallites to form AgCl, which consisted with the results characterized by XRD.

3.2.3. XPS

Figs. 6 and 7 show Ag3d and Y3d XPS spectra of the fresh catalyst (a), aged catalyst (b) and aged catalyst (c) with 125 ppm TCE in the feed gas. As shown in **Fig. 6**, the binding energies of Ag3d_{5/2} and Ag3d_{3/2} of the fresh catalyst (a) were 368.8 and 374.7 eV, respectively. The binding energies of Ag3d_{5/2} and Ag3d_{3/2} of the aged catalyst (b) were 368.3 and 374.3 eV, respectively. Compared with the binding energies of metallic Ag3d_{5/2} (367.9 eV) and Ag3d_{3/2} (373.9 eV), the presence of 0.1 wt% Y₂O₃ made these binding energies increase obviously. This was due to the electron interaction

between Y and Ag, and the electron of Ag was transferred to Y, which made Y negatively charged and Ag3d peaks shift to higher binding energy. The binding energies of Ag3d of the aged catalyst (b) were lower than those of the fresh catalyst (a), which indicated that the electron interaction between Ag and Y was weakened during the epoxidation reaction. Ag3d XPS spectra of the aged catalyst (c) were quite different from that of the fresh catalyst (a). Ag3d peaks were split into four peaks which binding energies located at 368.4, 369.2, 374.3 and 375.0 eV, respectively, which were higher than those of the aged catalyst (b). This was due to the electron interaction between Cl and Ag, and Cl withdrawing electrons from Ag, which made the electron density of Ag atoms nearby decrease and hence made Ag3d peaks shift to higher binding energy and Ag existence in higher oxidation states. This electron-withdrawing effect of Cl was beneficial to produce more electrophilic oxygen species to increase PO selectivity, which agreed well with those reported in the references [22,29,30]. A part of Ag of NaCl-modified Ag catalyst existed as cation, and high oxidation state of Ag was favorable to produce electrophilic oxygen species [29]. The presence of the subsurface layer of electropositive Ag atoms was a prerequisite to produce active sites where electrophilic oxygen atoms could be absorbed, which played an important role in the epoxidation of propylene [22]. Unpromoted, size-selected Ag₃ clusters and ~3.5 nm Ag nanoparticles on alumina supports can catalyze the epoxidation of propylene with only a negligible amount of carbon dioxide formation and with high activity at low temperatures, in which oxidized silver trimers are more active and selective for the epoxidation reaction because of the open-shell nature of their electronic structure [30].

As shown in Fig. 7, the binding energies of Y3d_{5/2} and Y3d_{3/2} of the fresh catalyst (a) were 151.9 and 157.8 eV, and were lower than those (Y3d_{5/2} 156.4 eV, Y3d_{3/2} 158.2 eV) of pure Y₂O₃ powder. The oxidation state of Y of the fresh catalyst (a) was lower than Y³⁺, that is to say, Y got electrons from Ag and thus the valence of Y and Ag should be 3- δ and δ^+ , respectively. Addition of Re led to Ag electron-deficient and Re⁷⁺ transforming to Re^{7- δ} over the modified Ag catalyst with Re for the epoxidation of ethylene [31]. The intensities of Y3d peaks of the aged catalyst (b) and aged catalyst (c) were weaker than those of the fresh catalyst (a), which indicated that Y₂O₃ moved into Ag crystallites to be detected by XPS or SEM-EDS with difficulty after reaction for 150 h. Therefore Y₂O₃ played a role of electron-type promoter that could strongly polarize electron cloud of nearby Ag, which made the absorbed oxygen species hold proper electrophilic character and then attack C=C bond of propylene to produce PO.

4. Conclusions

With an increase in the concentration of chlorohydrocarbon in the feed gas, PO selectivity increased significantly and propylene conversion decreased remarkably and then the catalytic performance remained nearly constant when the concentration of chlorohydrocarbon was more than 125 ppm. TCE had more positive effect on PO selectivity than DCE. When the concentration of TCE was 125 ppm, PO selectivity increased from 46.8% to 75.6% and propylene conversion declined from 4.0% to 0.77% after 10 h induction period, and then the catalytic performance remained nearly constant for 140 h. A small amount of TCE could effectively control

the surface morphology of the catalyst and restrain the agglomeration of Ag crystallites, in which TCE was dissociated on the surface of Ag crystallites to form AgCl and the coexistence of Ag and AgCl was favorable to increase PO selectivity. The presence of Cl could withdraw electrons from nearby Ag and thus make Ag electropositive, which was beneficial to produce more active sites where electrophilic oxygen species could be absorbed to increase PO selectivity. Y₂O₃ played a role of electron-type promoter that could strongly polarize electron cloud of nearby Ag, which made the absorbed oxygen species hold proper electrophilic character and then attack C=C bond of propylene to produce PO.

Acknowledgments

This project was supported by National Basic Research Program of China (2010CB732300), Commission of Science and Technology of Shanghai Municipality (09JC1404000), Program for New Century Excellent Talents in University (NCET-09-0343), Shu Guang Project of Shanghai Municipal Education Commission and Shanghai Education Development Foundation (10SG30).

References

- [1] K. Weissmehl, H.J. Arpe, Industrial Organic Chemistry, 4th ed., Wiley-VCH, Weinheim, Germany, 2003.
- [2] A.H. Tullio, P.L. Short, Chem. Eng. News 84 (2006) 22–23.
- [3] G. Blanco-Brieva, M.C. Capel-Sanchez, M.P. Frutos, A. Padilla-Polo, J.M. Campos-Martin, J.L.G. Fierro, Ind. Eng. Chem. Res. 47 (2008) 8011–8015.
- [4] T.A. Nijhuis, S. Musch, M. Makkee, J.A. Moulijn, Appl. Catal. A: Gen. 196 (2000) 217–224.
- [5] M.S. Stark, D.J. Waddington, Int. J. Chem. Kinet. 27 (1995) 123–151.
- [6] P. Dagaut, M. Cathonnet, J.C. Boettner, Combust. Sci. Technol. 83 (1992) 167–185.
- [7] R.D. Wilk, N.P. Cernansky, W.J. Pitz, C.K. Westbrook, Combust. Flame 77 (1989) 145–170.
- [8] V. Duma, D. Honicke, J. Catal. 191 (2000) 93–104.
- [9] Y. Wang, H. Chu, W.M. Zhu, Q.H. Zhang, Catal. Today 131 (2008) 496–504.
- [10] W.G. Su, S.G. Wang, P.L. Ying, Z.C. Feng, C. Li, J. Catal. 268 (2009) 165–174.
- [11] H. Chu, L.J. Yang, Q.H. Zhang, Y. Wang, J. Catal. 241 (2006) 225–228.
- [12] W.M. Zhu, Q.H. Zhang, Y. Wang, J. Phys. Chem. C 112 (2008) 7731–7734.
- [13] T.A. Nijhuis, M. Makkee, J.A. Moulijn, B.M. Weckhuysen, Ind. Eng. Chem. Res. 45 (2006) 3447–3459.
- [14] D.L. Trent, Kirk-Othmer Encyclopedia of Chemical Technology, vol. 20, 4th ed., Wiley, New York, 1996.
- [15] Z.M. Hu, H. Nakai, H. Nakatsuji, Surf. Sci. 401 (1998) 371–391.
- [16] M.A. Barteau, R.J. Madix, J. Am. Chem. Soc. 105 (1983) 344–349.
- [17] M. Akimoto, K. Ichikawa, E. Echigoya, J. Catal. 76 (1982) 333–344.
- [18] M. Imachi, M. Egashira, R.L. Kuczkowski, N.W. Cant, J. Catal. 70 (1981) 177–186.
- [19] P.V. Geenen, H.J. Boss, G.T. Pott, J. Catal. 77 (1982) 499–510.
- [20] G.J. Jin, G.Z. Lu, Y.L. Guo, Y. Guo, J.S. Wang, X.H. Liu, Catal. Today 93–95 (2004) 173–182.
- [21] G.J. Jin, G.Z. Lu, Y.L. Guo, Y. Guo, J.S. Wang, W.Y. Kong, X.H. Liu, J. Mol. Catal. A: Chem. 232 (2005) 165–172.
- [22] W. Yao, Y.L. Guo, X.H. Liu, Y. Guo, Y.Q. Wang, Y.S. Wang, Z.G. Zhang, G.Z. Lu, Catal. Lett. 119 (2007) 185–190.
- [23] W. Yao, G.Z. Lu, Y.L. Guo, Y. Guo, Y.Q. Wang, Z.G. Zhang, J. Mol. Catal. A: Chem. 276 (2007) 162–167.
- [24] G.Z. Lu, X.B. Zuo, Catal. Lett. 58 (1999) 67–70.
- [25] M.F. Luo, J.Q. Lu, C. Li, Catal. Lett. 86 (2003) 43–49.
- [26] M. Atkins, J. Couves, M. Hague, B.H. Sakakini, K.C. Waugh, J. Catal. 235 (2005) 103–113.
- [27] M. Bowker, K.C. Waugh, Surf. Sci. 134 (1983) 639–664.
- [28] G.B. Hoflund, D.M. Minahany, J. Catal. 162 (1996) 48–53.
- [29] J.Q. Lu, M.F. Luo, H. Lei, C. Li, Appl. Catal. A: Gen. 237 (2002) 11–19.
- [30] Y. Lei, F. Mehmood, S. Lee, J. Greeley, B. Lee, S. Seifert, R.E. Winans, J.W. Elam, R.J. Meyer, P.C. Redfern, D. Teschner, R. Schlögl, M.J. Pellin, L.A. Curtiss, S. Vajda, Science 328 (2010) 224–228.
- [31] J. Yang, J.F. Deng, X.H. Yuan, S. Zhang, Appl. Catal. A: Gen. 92 (1992) 73–80.